

# An analytic model for the prediction of wave setup, longshore currents and sediment transport on beaches with seawalls

Peter Ruggiero<sup>a,\*</sup>, William G. McDougal<sup>b,1</sup>

<sup>a</sup> Coastal Monitoring & Analysis Program, Washington Department of Ecology, PO Box 47600, Olympia, WA 98504-7600, USA

<sup>b</sup> Ocean Engineering Program, Oregon State University, Corvallis, OR 97331, USA

Received 18 February 2000; received in revised form 26 April 2001; accepted 1 May 2001

## Abstract

An analytic model is developed to predict the time- and depth-averaged cross-shore and longshore hydrodynamics as well as the longshore sediment transport on a planar beach backed by a seawall. Similar to the classical no seawall derivations of the problem, the model assumes shallow water, small angle of wave incidence, and spilling breakers. The reflected wave energy flux is conserved while the increased energy in the surf zone due to the reflected wave is assumed to be dissipated in the incident wave. A partial standing wave develops in front of the seawall causing modulations of the radiation stresses, the bottom stress, and the resulting wave setup, longshore current and longshore sediment transport. The influence of these modulations increases as the beach slope decreases due to a greater number of standing waves that develop across the wider surf zone. The total water depth slope (including wave setup) is steeper on a beach with a seawall than on a non-armored beach. Both the longshore current and the longshore sediment transport are strongly influenced by the cross-shore location of the seawall. On steep beaches, the total sediment transport is less than that for a natural beach. For milder sloped beaches, the modulations due to partial standing waves become significant and the transport may be either more or less than that for a beach with no wall, depending on the location of the seawall. These mixed results help to explain some of the confusion and contradictions found in the available seawall literature and may aid in focusing future research on the seawall problem. © 2001 Elsevier Science B.V. All rights reserved.

*Keywords:* Seawalls; Beaches; Wave setup; Longshore currents; Longshore sediment transport; Analytic model

## 1. Introduction

The effect that seawalls have on beaches has been a topic of considerable research and controversy for

many years and recent reviews of the available literature (Kraus, 1987; Griggs and Tait, 1990; Kraus and McDougal, 1996) have demonstrated the need for more study. Beaches have been reputed to respond to wave–seawall interactions in many ways including the formation of scour troughs, beach lowering, end scour, up-coast accretion, down-coast erosion, far down-coast shoals, reflection bars, delayed post-storm recovery, etc. Processes identified as having contributed to these possible responses include sedi-

\* Corresponding author. Tel.: +1-360-407-6230; fax: +1-360-407-6902.

E-mail addresses: prug461@ecy.wa.gov (P. Ruggiero), mcdougal@enr.orst.edu (W.G. McDougal).

<sup>1</sup> Tel.: +1-541-737-2804; fax: +1-541-737-3052.

ment impoundment (groin effect), removal of upland sand from the sediment budget, wave reflection, acceleration of longshore currents, increased sediment mobilization, and so on. Controls on how these processes affect beach change have also been discussed, long-term shoreline change (passive or background erosion), storm events (active erosion), position of the seawall relative to the surf zone, width of the surf zone, sediment supply as well as characteristics of waves and the seawall itself. Confusion and disagreement in the literature is compounded by the lack of sufficient field data and inconclusive physical and theoretical models.

It is generally accepted that on beaches experiencing passive erosion (for example, beaches eroding due to relative sea level rise), the beach fronting a seawall will eventually disappear. As just one example, armored shorelines in Oahu have been shown to cause narrowing and the loss of sandy beaches over an approximately 50-year period on a coast experiencing 1.55 mm/year of relative sea level rise (Fletcher et al., 1997). In contrast, three long-term field studies have recently documented seawall-backed beaches experiencing no significant negative impacts. These studies, in California (Griggs et al., 1994), Oregon (Hearon et al., 1996) and Virginia (Jones and Basco, 1996), each extend over time scales on the order of a decade. Measurable or significant differences between profiles for seawall-backed and non-armored beaches were not found in these studies, suggesting little long-term effect of seawalls on the beaches. These results are in part attributable to the position of the walls relative to mean sea level and the frequency and intensity with which they are impacted by waves. In both the California and Oregon studies, the walls were impacted only during the largest winter storm waves.

The above field studies suggest that seawalls do not inhibit the seasonal recovery of beaches, however, the short-term (storm event scale) influence of seawalls on sandy beaches (active erosion) is much more uncertain and is the source of much of the controversy surrounding seawalls. For example, the commonly accepted hypothesis that the reflection of normally incident waves from a seawall is a significant contributor to beach profile change, and to the development of a scour trench located in front of seawalls, has been recently cast into doubt. Several

numerical cross-shore profile models have been developed to examine this question, including a modified version of SBEACH, which explicitly includes wave reflection from the seawall and its influence on wave breaking and setup (McDougal et al., 1996). This study yielded two surprising results. The first is that the beach change predictions including reflected waves were not substantially different from those neglecting reflection (i.e. the standard SBEACH model with a no transport condition at the location of the seawall). The second was that a large scour trench did not always develop at the toe of the seawall, even for very energetic waves. These numerical results were confirmed in the large-scale model tests conducted as a component of the SUPERANK experiments (Kraus et al., 1992). The agreement of these two-dimensional numerical and physical models indicate that alongshore processes may be significant in event scale seawall-related effects (Kraus and McDougal, 1996).

Unfortunately, there is much less understanding of the alongshore processes in front of seawalls. In an unpublished doctoral dissertation, Jones (1975) theoretically and experimentally examined the effects of a seawall on longshore currents and the response of the fronting beach. He found that the longshore current profiles exhibited maxima and minima in response to a standing wave system that developed in front of the seawall. Maximum erosion was observed at the toe of the seawall, and the maximum net erosion occurred if the seawall was positioned approximately three-fifths of the distance from the breakpoint to the still water line. Silvester (1977) suggested that oblique wave incidence on a seawall could establish a short-crested wave system, which would amplify the transport of material over what would normally occur without the wall. The bed fronting the wall would scour, the immediate down drift section of coast would recede, and further down coast a shoal would develop beyond the influence of wave reflection. In a monitoring project of the effect of structures and water levels on bluff and shoreline erosion in Lake Michigan, Birkemeier (1980) provides one of the few quantitative measurements of longshore currents in front of a seawall. The southward moving current during a small storm was measured with dye tracers and was observed to be much larger in front of the wall than the adjacent

sections of coast. In a study based on 20 years of surveys along the Gold Coast, Australia, MacDonald and Patterson (1984) noted that “once the waves impinge on the seawalls for a significant proportion of the time, wave reflections and accelerated longshore currents can lead to increased scour adjacent to the walls.” In contrast, Dean (1986) argues that there is no factual data to support the contention that armoring causes increased sediment transport and thus a steepening of the beach profile. He presents a “rational” argument, based on the net longshore thrust including reflection, that wave reflection actually causes a reduction in longshore sediment transport. Plant and Griggs (1992) attempted to test the hypothesis that longshore currents in front of a seawall may be accelerated if the surf zone is sufficiently restricted by the presence of the wall. However, due to the logistics of their study site, they were unable to sample time periods long enough to resolve statistically meaningful variations in the mean current between walled and un-walled sections of beach.

Two recent studies provide the most detailed discussion of alongshore processes in front of seawalls available thus far, yet disagreement remains. Rakha and Kamphuis (1997a,b) developed a numerical model that included the effect of a seawall, its wave-transformation, wave-induced current, and morphology modules. Their numerical analyses, which were validated with small-scale physical model tests, suggested that seawalls had only a minor effect on both the longshore current and beach profile evolution. In fact, the volume of erosion for beaches backed by seawalls was nearly the same as that for a beach without a seawall. Miles et al. (2001) report on the first detailed field measurements of sediment transport processes in front of a seawall from an experiment on the south coast of England. During the relatively low energy conditions measured, both suspended sediment and longshore currents were observed to be stronger in front of a seawall than on an adjacent natural beach resulting in a longshore sediment transport rate that was on the order of a magnitude greater in front of the wall.

From the above often conflicting results, it is safe to say that it has not yet been confirmed in the field or the laboratory whether longshore currents and sediment transport rates will increase or decrease in

front of a seawall, as compared to a non-armored section of beach. This paper presents a simple analytic model to estimate longshore currents and littoral transport on planar beaches backed by seawalls, the objective being to better understand the influence of seawalls on nearshore processes. The model is based on the depth- and time-averaged equations of motion in the nearshore, assuming no longshore gradients. Once the waves, incident and reflected, and the total water depth including setup are determined, the longshore equation of motion is used to calculate a mean longshore current, and from this the sediment transport is estimated using a Bagnold-type transport model (Bagnold, 1963). This model is an extension of the classical no seawall derivations of wave setup, longshore currents and longshore sediment transport on planar beaches (e.g. Bowen et al., 1968; Bowen, 1969; Longuet-Higgins, 1970a,b; McDougal and Hudspeth, 1983a,b) and the standard assumptions are made. Attempts have been made, wherever possible, to compare the results of the McDougal and Hudspeth (1983a,b) no seawall results, hereinafter referred to as MH83, with the present model. This model is developed for a beach backed by an infinite vertical seawall located within the surf zone. The seawall must be located between the point of maximum setup on the beach face and the breaker line. Therefore, the model is valid for three of the six types of seawalls, Type-3, Type-4, and Type-5, described in Weggel's (1988) classification system based on the seawall's location with respect to the shoreline.

## 2. Wave model

As waves propagate toward the shore, they refract, shoal, and break. With a seawall present, they may also reflect, redirecting non-dissipated wave energy back through the surf zone. Changes in wave amplitude across the surf zone forces gradients in both the cross-shore and longshore radiation stresses. These gradients are balanced by an increase/decrease of the mean water level in the cross-shore (setup/setdown) and a bottom stress associated with the mean current in the longshore. Fig. 1A is a plan view definition sketch that illustrates the incident and reflected waves relative to the shoreline where  $\theta_i$

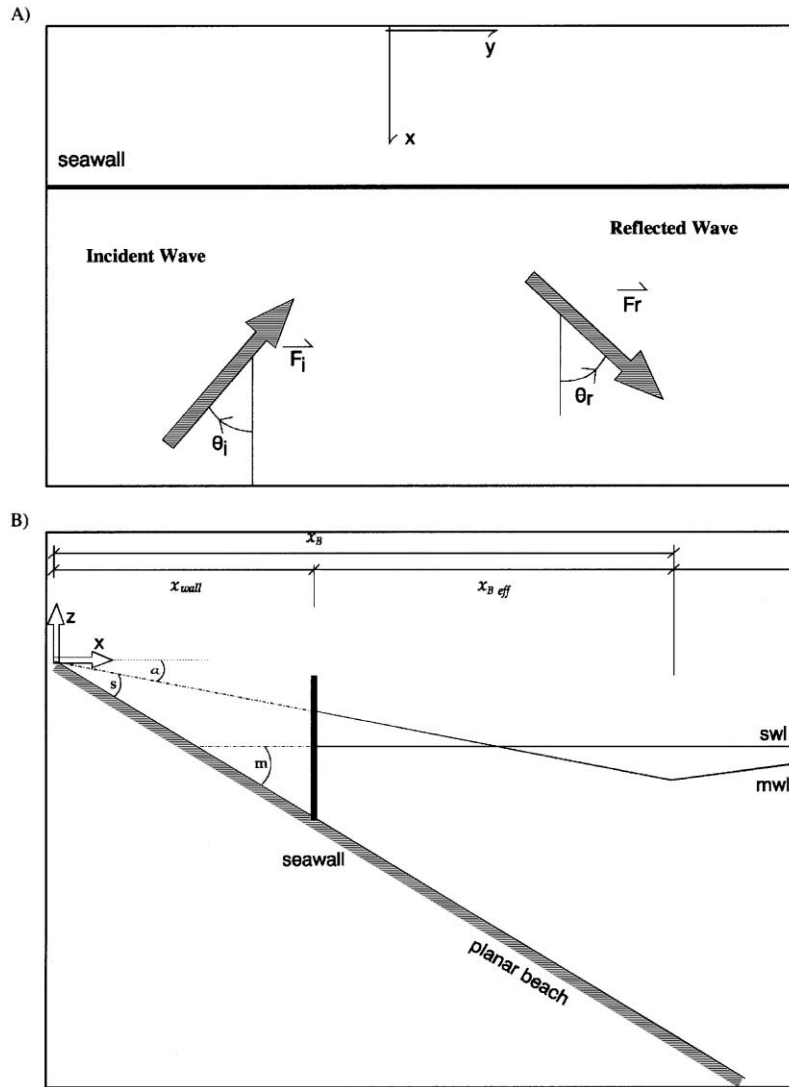


Fig. 1. (A) Plan view of the incident and reflected wave coordinate definitions and (B), profile view definition sketch of wave setup in front of a seawall.

is the incident wave angle,  $\theta_r$  is the reflected wave angle and the  $x$  coordinate is directed positive offshore with an origin landward of the seawall. This mathematically convenient choice of coordinate system will be discussed later. The reflected wave angle is related to the incident wave angle as  $\theta_r = -\theta_i$ , so hereafter, the angles will simply be denoted as  $\theta$  with the appropriate sign. A partial standing wave develops in front of the seawall in which the total

velocity potential can be expressed as the sum of the incident and reflected velocity potentials,

$$\begin{aligned} \Phi &= \phi_i + \phi_r \\ &= \frac{g \cosh k(d+z)}{\omega \cosh kd} [a_i \cos(kx \cos \theta - k y \sin \theta + \omega t) \\ &\quad + a_r \cos(kx \cos \theta + k y \sin \theta - \omega t + \varepsilon_r)] \end{aligned} \quad (1)$$

where  $g$  is the acceleration due to gravity,  $k$  is the wave number,  $d$  is the total water depth equal to the sum of the still water depth,  $h$ , and the mean free surface elevation  $\bar{\eta}$ ,  $a_i$  and  $a_r$  are the incident and reflected wave amplitudes, respectively,  $\omega$  is the angular frequency, and  $\varepsilon_r$  is the local phase between the incident and reflected waves and is a function of cross-shore location.

### 2.1. Incident and reflected wave amplitude

A seawall results in an additional source of energy in the surf zone as a result of wave reflection. Since the energy in the surf zone is saturated, the reflected wave causes the incident wave to begin breaking further offshore. This results in a redistribution of the incident energy dissipation due to the reflected wave. McDougal et al. (1996) assumed that this increase in dissipation took place within the incident wave and results from numerical model runs employing this assumption agreed well with SUPER-TANK laboratory results. Therefore, this assumption has been retained in the present work. The spilling breaker assumption is employed in the surf zone such that the envelope of the total breaker amplitude is related to the local total water depth as

$$a_i + a_r = \frac{\kappa}{2}(h + \bar{\eta}) = \frac{\kappa d}{2} \quad (2)$$

in which  $\kappa$  is a breaker index. Dissipation seaward of the breaker line is neglected and the cross-shore variation in the wave amplitude is determined assuming that the reflected wave energy flux,  $\vec{F}_r$ , is conserved across the surf zone

$$\vec{F}_r = \frac{1}{2} \rho g a_r^2 C_{gr} = \frac{1}{2} \rho g A \quad (3)$$

in which  $\rho$  is the water density,  $C_{gr}$  is the reflected wave group velocity and  $A$  is a constant. This constant is evaluated at the seawall

$$A = a_r^2 C_{gr} = a_{r_{wall}}^2 C_{gr_{wall}} \quad (4)$$

where the subscript  $(\cdot)_{wall}$  denotes values calculated at the seawall. The assumption that the increased energy in the surf zone, due to the reflected wave, is dissipated in the incident wave, allows Eqs. (2) and

(4) to be combined to give the cross-shore variation in the incident wave amplitude

$$a_i = \frac{\kappa d}{2} - \frac{A^{1/2}}{C_{gr}^{1/2}} \quad (5)$$

The constant  $A$  is determined from the reflected wave amplitude at the seawall, i.e. the incident wave amplitude at the seawall multiplied by a reflection coefficient,  $K_r$ . The reflected wave amplitude can now be defined as,

$$a_r = \left( \frac{K_r}{1 + K_r} \right) \frac{\kappa d_{wall}}{2} \left( \frac{C_{gr_{wall}}}{C_{gr}} \right)^{1/2} \quad (6)$$

This formulation is consistent with the work of Jones (1975), however, the present formulation also includes wave setup. Note that as  $K_r \rightarrow 0$ ,  $A \rightarrow 0$  and Eq. (5) collapses to the classical formulation for spilling breakers. Fig. 2A illustrates the cross-shore variation of the envelopes of both the incident and reflected wave amplitudes for a particular scenario in which the incident wave amplitude at the break point is 3.5 m, the wave period is 15 s, the beach slope is 1 V:100 H, and the seawall is located at 20% of the no wall surf zone width (case 3d, Table 1). Seaward of the break point, the incident wave amplitude is assumed constant. The dissipation of the no wall incident wave amplitude is shown for comparison, note that the break point is pushed seaward when the seawall is present.

### 2.2. Cross-shore equation of motion

Wave setup/setdown is determined from the cross-shore momentum equation, neglecting bottom and surface stresses and assuming no longshore gradients in morphology,  $\partial(\cdot)/\partial y = 0$ ,

$$-pg(h + \bar{\eta}) \frac{d}{dx} \bar{\eta} = \frac{d}{dx} S_{xx} \quad (7)$$

where  $S_{xx}$  is the onshore component of the onshore-directed radiation stress. The derivation of  $S_{xx}$  presented here includes the reflected wave and is slightly different from that of McDougal et al. (1996) in that the spatial derivatives of the phase between the incident and reflected wave,  $\varepsilon'_r$ , are derived analyti-

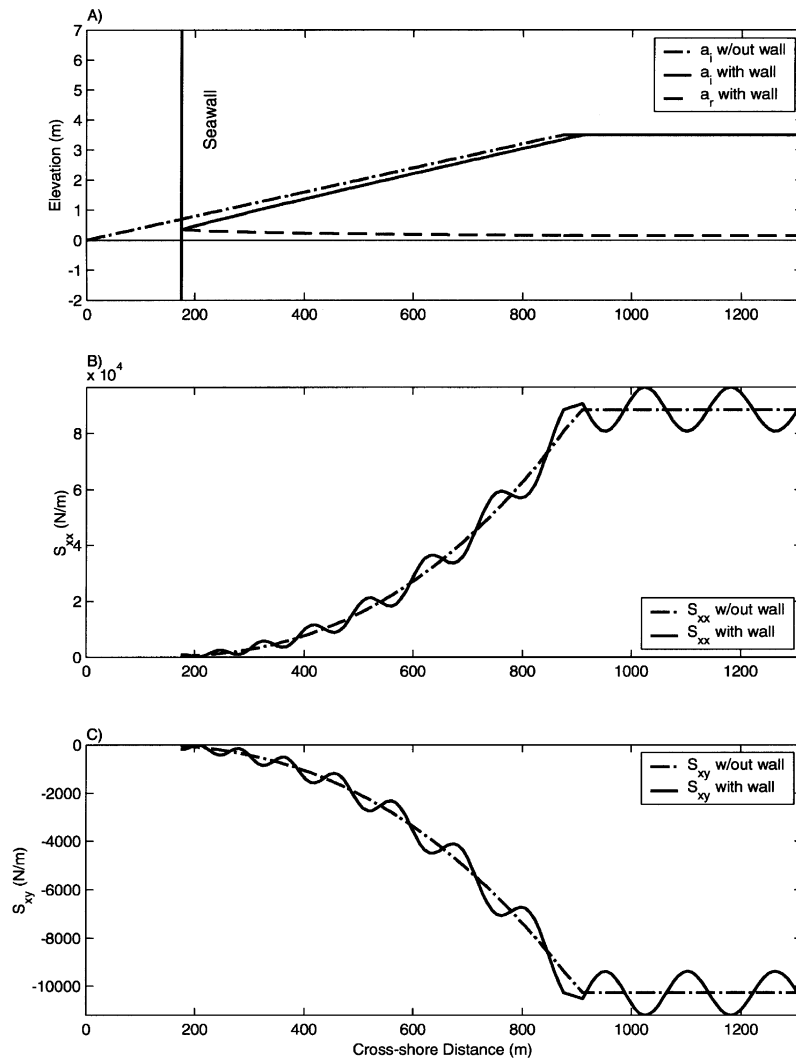


Fig. 2. Cross-shore variation of (A) incident and reflected wave amplitudes, (B) onshore component of the onshore directed radiation stress, and (C) alongshore component of the onshore directed radiation stress.

cally rather than computed via numerical iteration. The present result is written as

$$\begin{aligned}
 S_{xx} = & (E_{ii} + E_{rr}) \left[ n(\cos^2\theta + 1) - \frac{1}{2} \right] \\
 & + E_{ir} \cos(2kx\cos\theta + \varepsilon_r) [2n\sin^2\theta - 1] \\
 & + 4n \left[ \cos\theta (-E_{rr} + E_{ir} \cos(2kx\cos\theta + \varepsilon_r)) \right. \\
 & \left. + E_{rr} \right] \quad (8)
 \end{aligned}$$

where  $E_{ii}$  and  $E_{rr}$  are the incident and reflected wave energies,  $E_{ir}$  is given as

$$E_{ir} = \frac{1}{2} \rho g a_i a_r \quad (9)$$

and  $n$  is the ratio between the group velocity and the wave celerity. The formulation of the radiation stress as given in Eq. (8) is similar to the formulation used by Rakha and Kamphuis (1997a), however, here we

Table 1  
Range of wave conditions and beach slopes used in model runs

Case	$A_{iB}$ (m)	$T$ (s)	$m$
1 a,b,c,d	0.5	6	1:10, 1:20, 1:50, 1:100
2 a,b,c,d	1.5	10	1:10, 1:20, 1:50, 1:100
3 a,b,c,d	3.5	15	1:10, 1:20, 1:50, 1:100

have retained the local phase term between the incident and reflected waves as we are dealing with regular waves. The cross-shore variation of the on-shore component of the radiation stress is illustrated in Fig. 2B for the same input conditions as Fig. 2A. Due to the mild sloping beach, the modulations associated with the partial standing wave are clearly evident.

### 2.3. Solution technique

At this point, it is necessary to make several simplifying assumptions to develop an analytic solution to the cross-shore momentum equation. First, we assume shallow water in the region of interest and a planar beach with bottom slope  $m$ . In the classical solution to the depth- and time-averaged equations of motion (MH83), wave setup is a linear function of cross-shore location for a planar beach, while in the current work there is a spatial oscillation term,  $f = \cos(2kx\cos\theta + \varepsilon_r)$ , in the radiation stress that acts to modulate the time-averaged total depth. We will later show that a linear setup assumption is still a valid approximation for the determination of the longshore current and sediment transport in front of a seawall. Fig. 1B is a profile view of a seawall on a planar beach that suggests that the total water depth slope,  $s$ , is simply the bottom slope,  $m$ , less the slope of the wave setup,  $\alpha$ , in a coordinate system with an origin at the projected intersection of the wave setup with the no seawall planar beach. This choice of coordinate system allows the total depth to be written as  $d = sx$ , a convenience that greatly simplifies both the cross-shore and longshore equations of motion.

The wavelength is the product of the wave celerity,  $C$ , and the wave period,  $T$ , so with the above assumptions, the wave number may be written as

$$k = \frac{2\pi}{L} = \frac{2\pi}{CT} = \frac{\omega}{(gsx)^{1/2}} \tag{10}$$

in which  $L$  is the wavelength. It is assumed that refraction is sufficient to yield small breaking angles, and that once inside the surf zone, the change in wave angle is also small such that  $\theta \cong \theta_B$  the angle evaluated at the breaker line. The phase term in Eq. (8) can be separated into two parts,

$$\varepsilon_r = \varepsilon_{rw} + \varepsilon_{rg} \tag{11}$$

where  $\varepsilon_{rw}$  is determined by the amount of time it takes the incident wave to propagate from an arbitrary offshore location,  $x_o$ , to the seawall and back again to  $x_o$ .

$$\varepsilon_{rw} = \frac{4\pi}{T} \int_{x_o}^{x_{wall}} \frac{dx}{C\cos\theta} \tag{12}$$

A geometric phase  $\varepsilon_{rg}$  arises from the choice of coordinate system and is chosen to ensure an antinode at the seawall. The radiation stress term can now be simplified and combined with Eq. (7) to give the dimensional equation for wave setup

$$\frac{d\bar{\eta}^*}{dx^*} = \frac{-3}{4d^*} \frac{d}{dx^*} (a_1^{2*} + a_r^{2*} + 2a_1^* a_r^* f) \tag{13}$$

where the asterisks, which have been left off until this point for brevity, now denote dimensional quantities. Through introducing the following dimensionless quantities  $\bar{\eta} = \bar{\eta}^*/d_B^*$ ,  $X = x^*/x_B^*$ ,  $A = A^*T^*/(d_B^{*3}(2\pi)^{1/2})$ , and  $\omega = \omega^*(2\pi)^{1/2}$ , the cross-shore equation of motion can be integrated to give the non-dimensional spatial structure of the wave setup

$$\begin{aligned} \bar{\eta} = & -\frac{3\kappa^2 X}{8} - \frac{A\gamma^{1/2}}{2X} - \frac{9A^{1/2}\kappa\gamma^{1/4}}{4X^{1/4}} + \frac{3A\gamma^{1/2}f}{2X^{3/2}} \\ & - \frac{3A^{1/2}\kappa\gamma^{1/4}f}{4X^{1/4}} + \frac{3A\gamma^{1/2}}{4} \int X^{-5/2} f dX \\ & - \frac{3A^{1/2}\kappa\gamma^{1/4}}{4} \int X^{-5/4} f dX + c_1 \end{aligned} \tag{14}$$

where  $\gamma = d_B^*/L_0^*$ ,  $L_0^* = g^*T^{*2}/(2\pi)$  is the deep-water wavelength from linear wave theory, and  $c_1$  is a constant of integration. The two integrals in Eq. (14) have been evaluated, and result in lengthy expressions that are reported in Ruggiero (1997). Wave setdown can be derived and non-dimensionalized in a similar manner to that described for the setup and

then the constant  $c_1$  is determined by matching the setup and setdown at the breaker line. Once again, with no reflection from the seawall,  $A \rightarrow 0$  and Eq. (14) collapses to the classical, MH83, no seawall formulation for wave setup on a planar beach.

#### 2.4. Influence of seawall in the cross-shore

The seawall, and the partial standing wave that develops in front of it, affect cross-shore surf zone dynamics in several ways. Table 1 lists the range of wave conditions and beach slopes that have been used to demonstrate the behaviour of the model, a sensitivity analysis that ranges from dissipative to reflective beaches and from mild to storm conditions. With 12 combinations of wave amplitude, wave period, and beach slope, the position of the seawall across the surf zone has been varied resulting in a total of 88 scenarios that have been examined. Fig. 3 demonstrates the influence of the seawall on the width of the surf zone. The ordinate is the ratio of the seawall location,  $x_{\text{wall}}$ , to the break point location  $x_{B \text{ no wall}}$ , calculated for a beach with the same still water depth slope,  $m$ , but with no seawall. This

scaling is chosen since it is not a priori known where waves will break due to the reflected waves from the seawall. The top curve represents the ratio of the break point calculated for the beach with the seawall,  $x_B$ , to  $x_{B \text{ no wall}}$ . The energy that is reflected back through the surf zone causes incoming waves to break further seaward than they would if no seawall was present. For example, a seawall located at approximately 50% of the no wall surf zone width causes waves to break 20% further seaward. The bottom curve demonstrates that the seawall does, however, reduce the effective width of the surf zone by eliminating the area behind the wall from the surf zone. For the same example, the effective width of the surf zone with the seawall is approximately 70% of the no wall surf zone width.

Fig. 4 shows three non-dimensional setup/setdown profiles representing three seawall locations, 20%, 40% and 60% of  $x_{B \text{ no wall}}$ . Unfortunately, in the non-dimensionalization of the cross-shore equations of motion (Eq. (14)), most wave parameters do not drop out of the solution as they do in no seawall setup/setdown models, i.e. MH83, but are retained in the non-dimensional terms  $\gamma$  and  $A$ . Rather than

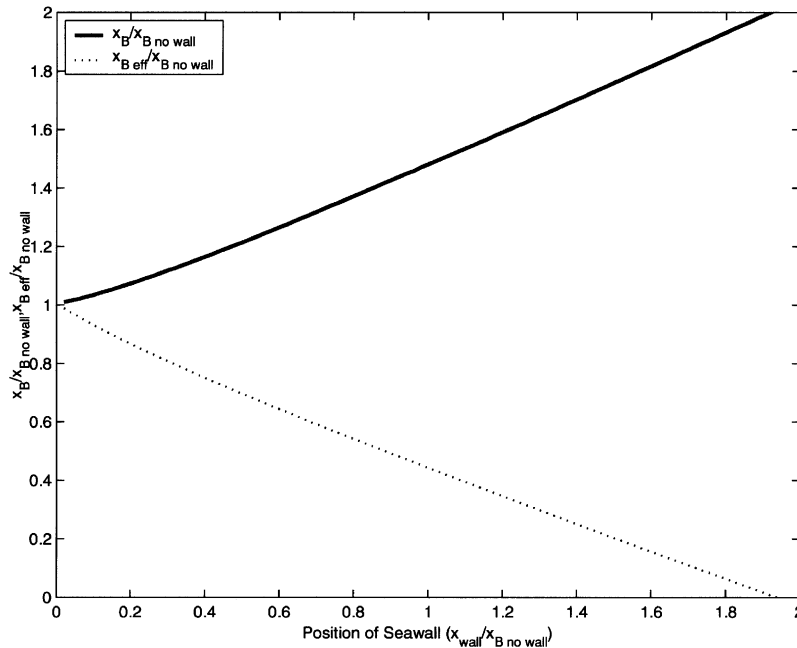


Fig. 3. Influence of a seawall on the surf zone width.

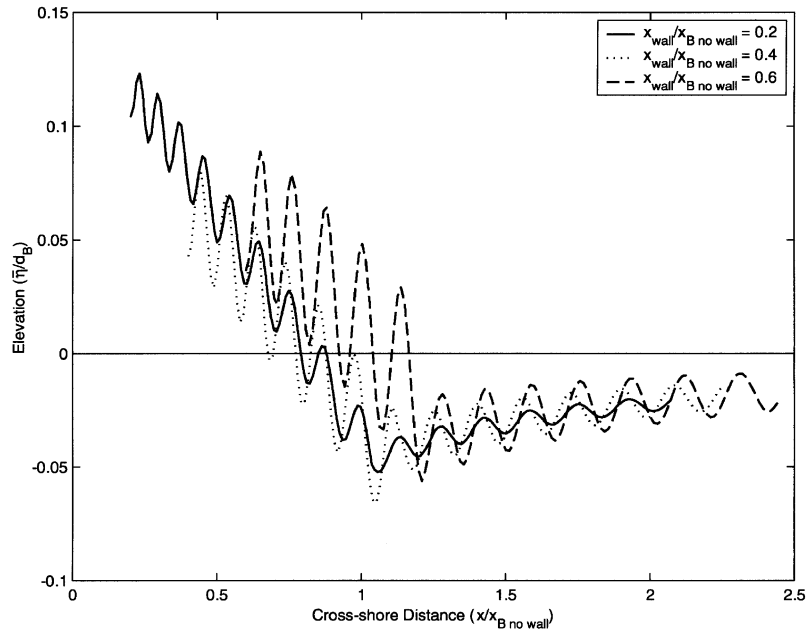


Fig. 4. Wave setup/setdown in front of seawall for three locations of the seawall,  $x_{\text{wall}}/x_{B \text{ no wall}} = 0.2$  (solid line), 0.4 (dotted line) and 0.6 (dashed line).

performing model sensitivity analyses with these non-physical parameters, specific dimensional input parameters have been used to generate a wide range of model output. Therefore, Fig. 4 is not general, but represents a set of conditions from Table 1; case 3d with  $a_{iB} = 3.5$  m,  $T = 15$  s, and  $m = 1$  V:100 H. This example consists of storm conditions on a dissipative beach and has several partial standing waves in the surf zone. The spatial oscillation term causes the modulation in the wave setup/setdown with the number of oscillations across the surf zone depending on the ratio of the wavelength to the surf zone width. Similar wave setup profiles were reported by Rakha and Kamphuis (1997a). Miles et al. (2001) noted that their in situ measurements in front of a seawall were positioned within a nodal structure but unfortunately measurements were made at only one cross-shore location and the standing structure was unresolved. Fig. 4 also reveals that the magnitude of these modulations increases as the seawall is moved seaward. This is because the incident wave at the seawall is larger, and therefore the reflected wave is also larger. To further illustrate the seaward extension of the surf zone due to the waves reflected from

the seawall, the cross-shore distance in Fig. 4 has again been scaled by  $x_{B \text{ no wall}}$ , rather than by  $x_B$  which would have set each of the scaled break points to a value of 1.

As discussed earlier, a simple representation of the total water depth is required to solve the longshore equations of motion analytically. To validate the assumption of a linear total water depth slope, i.e.  $d = sx$ , 88 setup profiles were calculated using the cases of Table 1 and a varying seawall position. These results were then used to determine the corresponding still water depth profiles from the assumed planar total water depth. Fig. 5 shows a composite of both the wave setup and the projected bottom profiles generated from the model. The excellent correlation that a planar bottom slope has with the model results ( $r^2 = 0.99$ ) verifies that the modulation of the wave setup has only a small effect on the total water depth, thus the approximation of a linear total water depth slope is reasonable. The linear regression gives a relationship between the total slope  $s$ , and the bottom slope  $m$  of the planar beach,  $s = 0.84 m$ , that is necessary in solving the longshore equation of motion. For comparison, an analytic solution is pos-

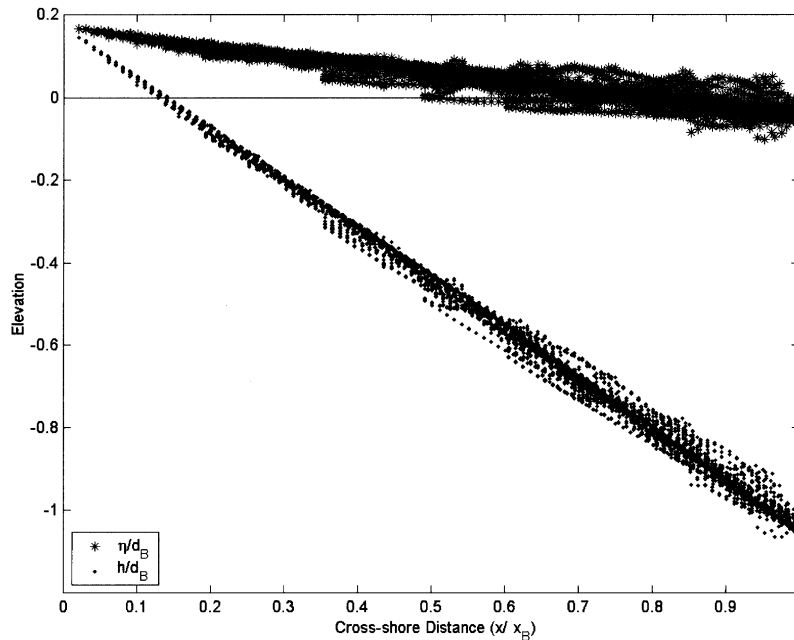


Fig. 5. Composite of 88 non-dimensional setup and still water depth profiles. Results of linear regression gives  $h/d_B = 0.156 - 1.197X$ ,  $r^2 = 0.995$ .

sible for the no seawall total depth slope and therefore a relationship between  $s_{MH83}$  and  $m$  for a beach with no seawall

$$S_{MH83} = m \left( 1 - \frac{3\kappa^2}{8 + 3\kappa^2} \right). \quad (15)$$

For a typical mild slope breaker index of  $\kappa = 0.8$ , this gives  $s_{MH83} = 0.81m$ . Therefore, the total water depth slope is slightly steeper for a beach with a seawall than for a beach without a seawall. This indicates that the decrease in effective surf zone width has more affect on the total slope than the seaward translation of the break point.

### 3. Longshore current

Most theories for mean longshore currents due to oblique wave approach are based on a longshore momentum flux balance (Bowen, 1969; Longuet-Higgins, 1970a,b; Thornton and Guza, 1986 and MH83). The present model follows this tradition, and includes the effect of reflected waves from a

seawall. The time-averaged equation for longshore momentum can be simplified to a balance between the cross-shore gradient of the longshore radiation stress and the bottom stress. An eddy viscosity term modeling surf zone turbulence is included, serving to smooth the mean longshore current. The balance becomes

$$\frac{d}{dx} \left( \mu_e d \frac{d}{dx} \nu \right) + \tau_{by} = \frac{d}{dx} S_{xy} \quad (16)$$

where  $\mu_e$  is the eddy viscosity,  $\nu$  is the mean longshore current,  $\tau_{by}$  is the bottom stress in the longshore direction,  $S_{xy}$  is the longshore component of the onshore radiation stress and again asterisks denoting dimensional quantities will be left off for brevity until the solution technique is presented. The eddy viscosity term is necessary for a reasonable longshore current profile when the forcing is from monochromatic waves. Many eddy viscosity models have been proposed, but the longshore current is rather insensitive to the choice (McDougal and Hudspeth, 1986). We will assume a simple representation of  $\mu_e$  that increases linearly across the surf zone and

is proportional to a characteristic density, velocity and length scale

$$\mu_e = N\rho(gd)^{1/2}x \quad (17)$$

where  $N$  is a dimensionless constant.

### 3.1. Bottom stress

The bottom stress is estimated using a quadratic bottom shear stress law, based on the combined wave orbital velocity and mean current velocity

$$\tau_b = -\rho c_f |\vec{u}| \vec{u} \quad (18)$$

where  $c_f$  is a dimensionless coefficient and  $\vec{u}$  is the depth-averaged velocity vector. For a small angle of wave incidence and weak mean longshore current, the time-averaged bottom stress in the longshore direction can be written as

$$\tau_{by} = -\frac{1}{d} \int_{-d}^0 \rho c_f |u_x| (u_y + v) dx. \quad (19)$$

The longshore component of the wave orbital velocity,  $u_y$ , which is easily derived from Eq. (1), is proportional to  $\sin\theta$  and will be neglected from the bottom stress due to the small angle assumption. The onshore component of the wave orbital velocity including the reflected wave is

$$\begin{aligned} u_x = & \frac{gk \cosh k(d+z)}{\omega \cosh kd} \\ & \times \left( a_i \cos\theta \sin(kx \cos\theta - ky \sin\theta + \omega t) \right. \\ & + a_r \left( \cos\theta + \frac{\varepsilon'_r}{k} \right) \sin(kx \cos\theta \\ & \left. + ky \sin\theta - \omega + \varepsilon_r \right). \end{aligned} \quad (20)$$

After several trigonometric and algebraic simplifications, Eq. (20) can be re-written as

$$u_x = c_2 \sin[\omega t + \sigma(x)] \quad (21)$$

where the coefficient  $c_2$  is

$$\begin{aligned} c_2 = & g(z) \left( a_i^2 \cos^2\theta + 2a_i^2 \left( \cos\theta + \frac{\varepsilon'_r}{k} \right) \right. \\ & \left. - 2a_i a_r \cos\theta \left( \cos\theta + \frac{\varepsilon'_r}{k} \right) f \right)^{1/2} \end{aligned} \quad (22)$$

in which

$$g(z) = \frac{gk \cosh k(d+z)}{\omega \cosh kd} \quad (23)$$

and  $\sigma(x)$  is a spatially dependent phase term, which will be eliminated during the subsequent time averaging of the bottom stress. The coefficient  $c_2$  can be simplified via a binomial expansion, assuming  $a_r/a_i < 1$

$$c_2 \approx g(z) \cos\theta \left( a_i - a_r \left( 1 + \frac{\varepsilon'_r}{\cos\theta} \right) f \right). \quad (24)$$

This assumption is reasonable over most of the surf zone except very close to the wall. At the wall itself, if  $K_r = 1.0$ , the ratio  $a_r/a_i = 1$  and the simplified  $c_2$  would have the greatest error. This maximum error is approximately 14% at the seawall, and much less for the rest of the profile. Making the same set of assumptions as when determining the total water depth, depth and time averaging, the bottom stress becomes

$$\tau_{by} = -\frac{\rho c_f g}{\pi (gd)^{1/2}} (a_i + a_r f) v. \quad (25)$$

This formulation of the bottom stress contains the influence of the partial standing waves through the spatial oscillation term  $f$ . As with the effect of the modulations of the setup on the total water depth, the effect of the spatial oscillation term on the longshore current is also small. The bottom stress is significantly simplified by the approximation  $a_i + a_r f \approx \psi kd/2$  where  $\psi$  is a constant, giving

$$\tau_{by} = -\frac{\rho c_f \psi}{\pi} \kappa (gd)^{1/2} v. \quad (26)$$

This approximation is the same formulation of the bottom stress found in many of the no seawall solutions to the longshore equations of motion (MH83). The third, and final, manifestation of the spatial oscillation term has been retained and is in the forcing of Eq. (16),  $dS_{xy}/dx$ .

### 3.2. Longshore radiation stress

The longshore component of the onshore-directed radiation stress,  $S_{xy}$ , is derived accounting for the

partial standing wave, which develops in front of the seawall and can be written as

$$S_{xy} = n[(-E_{ii} + E_{rr})\sin\theta\cos\theta - 2(E_{ir}f + E_{rr})\sin\theta]. \quad (27)$$

Once again the cross-shore variation of this parameter is illustrated (Fig. 2C) in order to illustrate the fundamentals of the model. Note that the partial standing wave (case 3d) serves to modulate the radiation stress around the no wall formulation. Employing Snell's law for wave refraction and making the same set of assumptions as above, the cross-shore derivative of Eq. (27) is

$$\begin{aligned} \frac{d}{dx}S_{xy} &= \rho g \frac{\sin 2\theta}{4(gd_B)^{1/2}} \frac{d}{dx} [(-a_i^2 + a_r^2)(gd)^{1/2}] \\ &+ \rho g \frac{\sin 2\theta}{(gd_B)^{1/2}} (-a_i a_r f - a_r^2)(gd)^{1/2}. \end{aligned} \quad (28)$$

Gradients in the momentum flux are due to dissipation in wave energy across the surf zone and are assumed to be zero outside of the breaker line.

### 3.3. Solution technique

The dimensional equation (asterisks again imply dimensional quantities) for the longshore current in front of a seawall can now be written as

$$\begin{aligned} x^{*2} \frac{d^2 v^*}{dx^{*2}} + \frac{5}{2} x^* \frac{dv^*}{dx^*} - \frac{v^*}{P'} \\ = \frac{1}{(\rho^* N s (g^* s x^*)^{1/2})} \frac{dS_{xy}^*}{dx^*}, \end{aligned} \quad (29)$$

where the lateral mixing coefficient,  $P'$  is a constant similar to classical formulations of the problem (MH83). After non-dimensionalizing Eq. (29) in the same manner as the cross-shore equation of motion and expanding the radiation stress term, the non-di-

mensional longshore equation of motion can be written as

$$\begin{aligned} X^2 \frac{d^2 v}{dx^2} + \frac{5}{2} X \frac{dv}{dX} - \frac{v}{P'} \\ = c_3 X + c_4 X^{-1/4} + c_5 X^{-1/4} f + c_6 X^{3/4} f' \\ + c_7 X^{-1/2} f; \end{aligned} \quad (30)$$

where

$$\begin{aligned} c_3 &= -\frac{5\sin 2\theta \kappa^2 C_B}{32N}; \\ c_4 &= \frac{5\sin 2\theta \kappa A^{1/2} \gamma^{1/4} C_B}{16N}; \\ c_5 &= -\frac{5\sin 2\theta \kappa A^{1/2} \gamma^{1/4} C_B}{8N}; \\ c_6 &= -\frac{5\sin \theta \kappa A^{1/2} \gamma^{1/4} C_B}{2N}; \\ c_7 &= -\frac{\sin \theta A \gamma^{1/2} C_B}{N} \end{aligned} \quad (31)$$

and  $C_B = (g^* d_B^*)^{1/2} / v_{B \text{ no wall}}^*$  is a non-dimensional break point celerity. The above expression contains four new terms beyond the classical (MH83) solution resulting from the inclusion of the reflected wave. Note that two of the terms in Eq. (31),  $c_4$  and  $c_7$ , are positive and act in the opposite direction of the main driving term,  $c_3$ . This effect of the seawall results from not all of the energy of the incoming waves being expended both due to backwards shoaling and refraction of the reflected waves. There are, however, two additional terms due to the presence of the seawall,  $c_5$  and  $c_6$ , which act with the main driving term of Eq. (31).

Eq. (30) is the Euler equation with the standard homogeneous solution and a particular solution determined via the method of undetermined coefficients. Due to the complicated forcing terms in Eq. (30),  $P'$  must be chosen carefully to give values for which the integrals arising from the solution technique can be solved. This is not a severe limitation in that the longshore current can still be solved over a range of  $P'$  values consistent with what is usually employed in longshore current simulations. In the

subsequent discussion of the model results, solutions with  $P' = 0.4$  are presented. Once again, note that as  $K_r \rightarrow 0$ , Eq. (30) collapses to the no seawall formulation of longshore currents on a planar beach. Boundary conditions must be introduced to evaluate the integration constants. The velocity must be bounded far offshore and the velocity and the gradient of the velocity must match at the breaker line. Typically, in longshore current models, the velocity must also be bound at the shoreline. In the present model, with wave reflection off of a seawall, a mixed boundary condition is chosen that allows for a no-slip wall condition, free-slip wall condition, or a combination of the two. The free-slip condition is the only boundary condition for which results are discussed below.

### 3.4. Influence of a seawall in the alongshore

With a model for wave setup, and the longshore equation of motion solved, the longshore current in front of a seawall can now be calculated. As with the cross-shore equation of motion, non-dimensionalizing does not sufficiently reduce the number of pa-

rameters to develop generic plots, so individual cases must be analyzed resulting in rather cumbersome sensitivity analyses. Fig. 6 shows the non-dimensional longshore current in front of a seawall for case 3d (storm conditions on a dissipative beach) with the seawall located at several positions across the surf zone. As found by Jones (1975), local maxima and minima are evident in the longshore current profiles due to the partial standing waves which develop in front of the seawall. The magnitudes of the longshore currents are sensitive to the position of the seawall, and in the present case, the largest current is found when the seawall is approximately three-fifths of the way across the surf zone. The MH83 solution is also shown in Fig. 6 as the thick solid line illustrating that the position of the seawall determines whether or not the longshore current with a seawall is greater than or less than the longshore current on a similar beach with no wall. This dependency on relative seawall location confirms a hypothesis that has been suggested by many researchers (e.g. Dean, 1986; Weggel, 1988; Griggs and Tait, 1990).

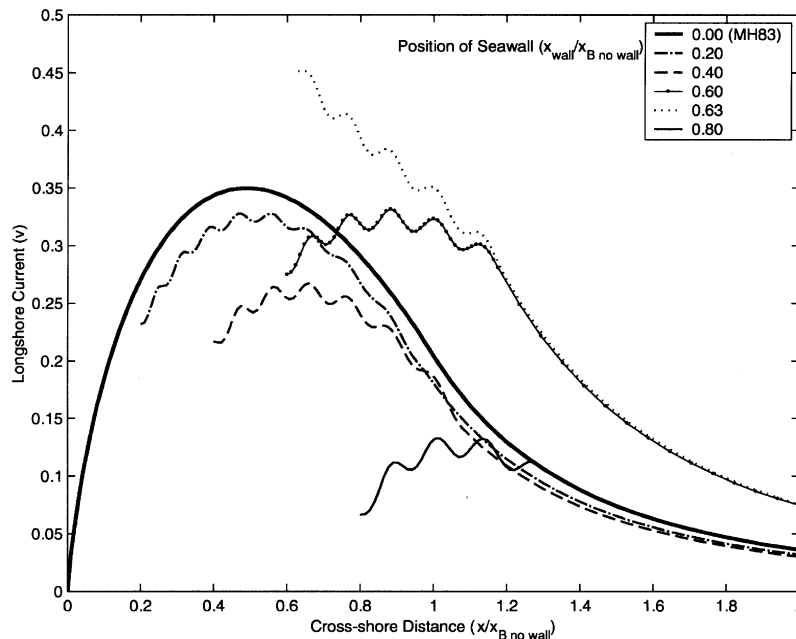


Fig. 6. Longshore current profiles fronting a seawall for model case 3d and several positions of the wall,  $x_{\text{wall}}/x_{B \text{ no wall}} = 0.2$  (dash-dot line), 0.4 (dashed line), 0.6 (small dots on thin solid line), 0.63 (dotted line) and 0.8 (thin solid line). The thick solid line represents the classical longshore current solution with no seawall.

Fig. 6 was generated for a single beach/wave condition and five positions of the seawall and similar results have been generated for many other conditions. The model substantiates the observation made by Weggel (1988) that “reflected waves alter radiation stresses and thus affect the cross-shore distribution of longshore current velocity in front of the wall”. However, the behaviour of the longshore current profiles is quite complex, suggesting that integrated quantities across the surf zone might be simpler to analyze. Fig. 7 illustrates the results of many model runs in which the total dimensionless longshore current has been integrated from the seawall

out to an offshore location of five times the break point to yield the total alongshore volumetric flow rate,  $Q_{tot}$ . In all cases, the longshore current asymptotically reaches zero well landward of five surf zone widths ensuring that the above integration is robust. Each panel in Fig. 7 represents one beach slope, three offshore wave conditions, and many positions of the seawall ranging from 20% to 80% of the no wall surf zone width. Fig. 7A, the steepest beach (1 V:10 H), shows a fairly simple response to the location of the seawall. The total volumetric flow rate decreases as the wall is moved seaward until the wall is approximately 70% of the way across the no

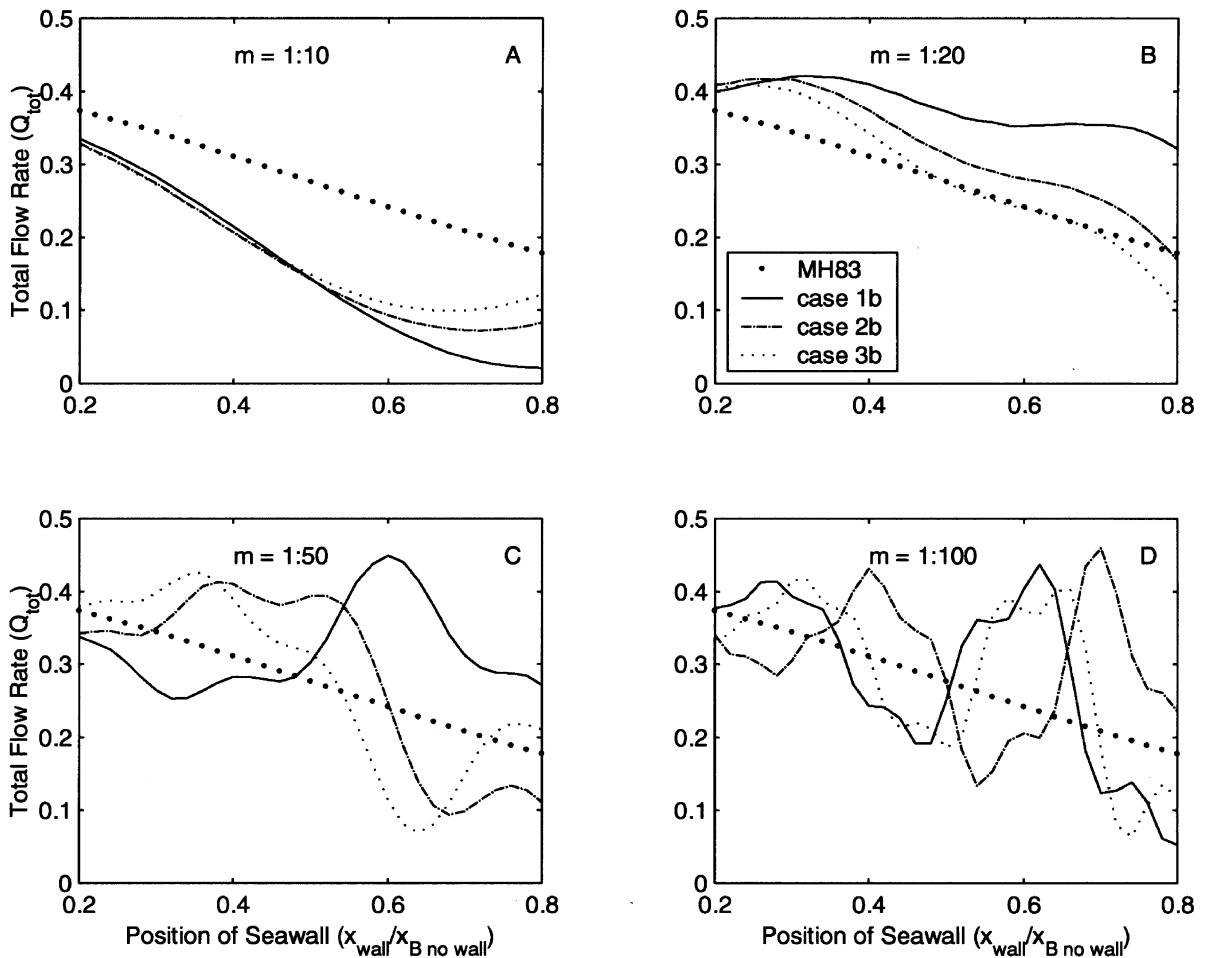


Fig. 7. Total volumetric flow rate fronting a seawall for four planar beach slopes, (A)  $m = 1:10$ , (B)  $m = 1:20$ , (C)  $m = 1:50$ , (D)  $m = 1:100$ , and several wave conditions, case 1 (solid line), 2 (dashed-dot line) and 3 (small dotted line). The large dots represent the total volumetric flow rate with no seawall.

seawall surf zone and then the total flow begins to increase. This steep beach sharply reduces the amount of longshore current as compared to a beach without a seawall. This is primarily due to the phase of the standing wave that has a larger wavelength than the surf zone width. Fig. 7B reveals that a moderately sloped beach (1 V:20 H) increases the longshore current relative to a beach with no wall. Interestingly, the larger wave heights and longer wave periods force less total flow than the smaller waves, again due to the phase of the partial standing wave relative to the surf zone width. The next two panels, for mild slopes of 1 V:50 H (Fig. 7C) and 1 V:100 H (Fig. 7D), have many inflection points, clearly demonstrating the strong dependence of the longshore current on the cross-shore position of the seawall in the surf zone.

#### 4. Longshore sediment transport

Once the longshore current in front of a seawall is known, an estimate of the longshore sediment transport profile is possible. A Bagnold-type energetic

model (Bagnold, 1963) is used which includes both bed load and suspended load. The model assumes that the orbital wave motion mobilizes the sediment, wave power is expended maintaining the sediment in motion, and the presence of a mean current, regardless of how small, transports the sediment. In calculating the sediment transport, the same set of assumptions is employed as when determining the wave setup and the longshore current. Non-dimensionalizing the transport rate by the no seawall, no mixing transport rate evaluated at the breaker line, the dimensionless transport,  $I$ , is given as (MH83)

$$I = \left( \frac{d_B}{d_{B \text{ no wall}}} \right)^2 XV. \tag{32}$$

Fig. 8 shows the non-dimensional sediment transport profile in front of a seawall for case 3d and the same positions of the seawall which were presented in Fig. 6. Similar to the response of the longshore current model, the magnitudes of sediment transport depend greatly on the position of the seawall. Modulation in the cross-shore structure of the sediment transport rate profile is again evident due to the

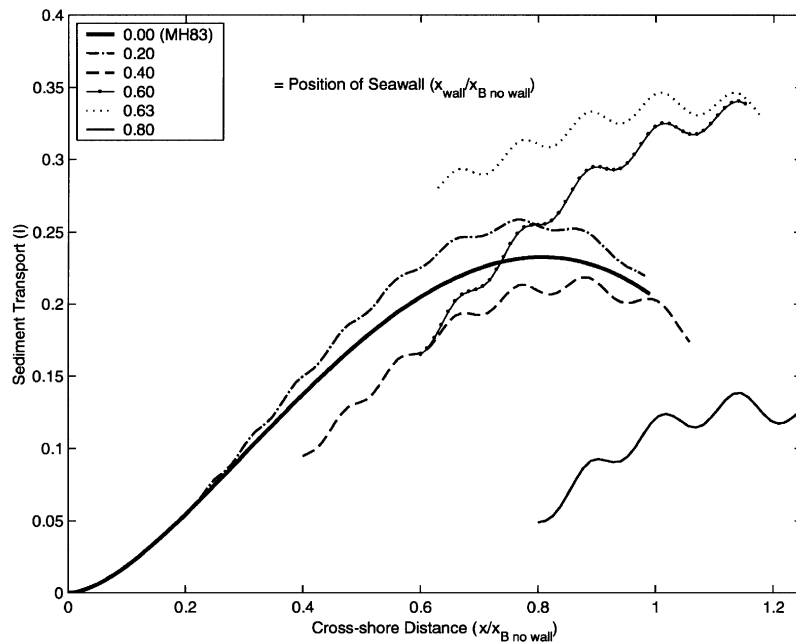


Fig. 8. Sediment transport profiles fronting a seawall for model case 3d and several positions of the wall,  $x_{wall}/x_{B \text{ no wall}}$ . Symbols are the same as Fig. 6.

partial standing wave in the surf zone. To test model sensitivity, integrated surf zone quantities are again analyzed. Fig. 9 reveals the dependency of the total quantity of sediment transport,  $I_{tot}$ , as a function of bottom slope, wave conditions, and the position of the seawall.  $I_{tot}$  is calculated by integrating the transport from the position of the seawall to the break point. Here, the integration stops at the break point because the sediment transport model is only valid in the surf zone. Due to the simplicity of the sediment transport model, the integrated sediment transport responds similarly to the integrated longshore current. For steep beaches, the total longshore

transport is less than that on a beach without a seawall. On moderately sloped beaches, the total transport is greater than a beach without a seawall. For mild sloped beaches, the total transport is generally greater with a seawall, but depends on the surf zone width relative to the number of standing waves within the surf zone.

Fig. 10 demonstrates the effect the reflection coefficient,  $K_r$ , has on the total sediment transport using wave case 3 from Table 1. For the mild slope (Fig. 10A), decreasing the reflection coefficient reduces the magnitude of the oscillations in the response due to a smaller standing wave system in the

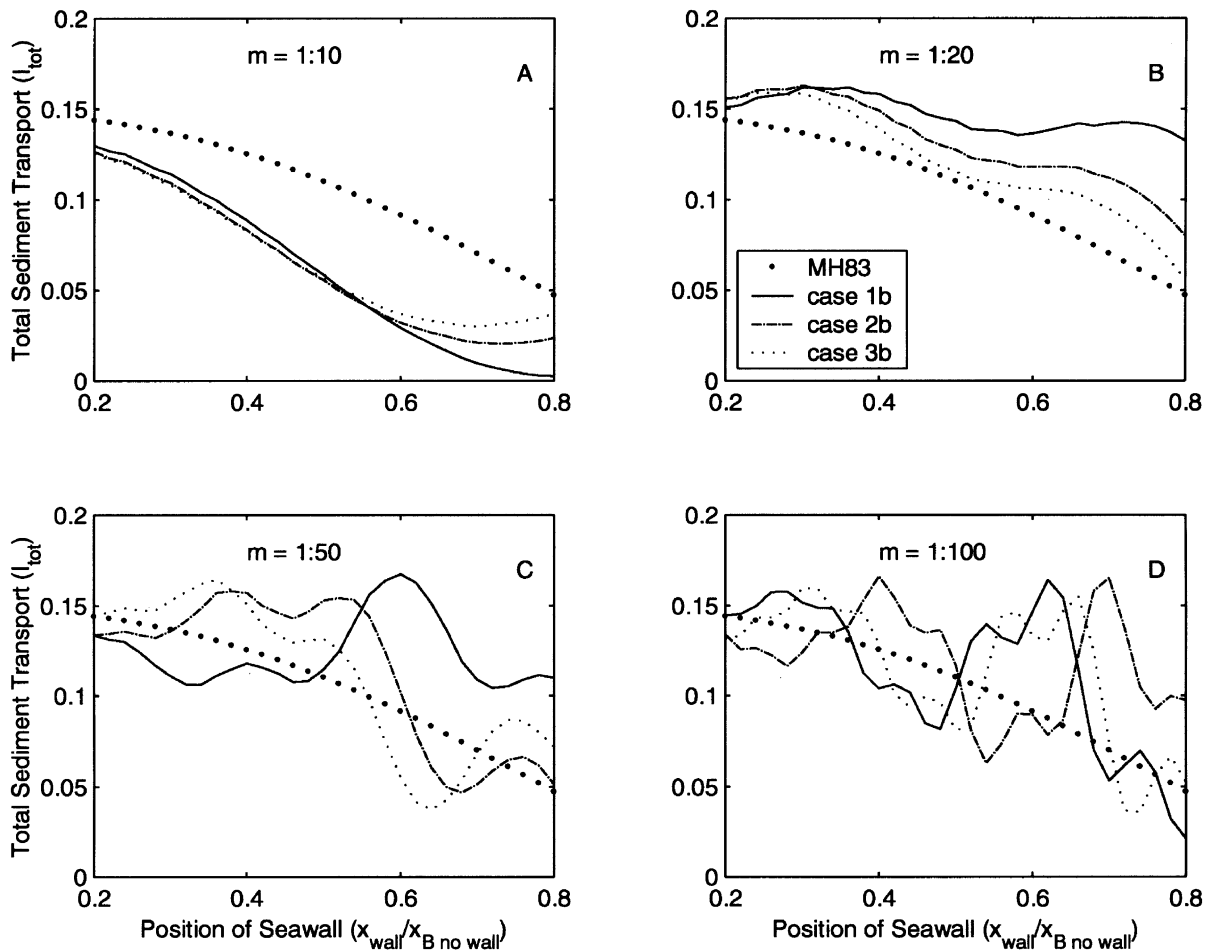


Fig. 9. Total sediment transport fronting a seawall for four planar beach slopes, (A)  $m = 1:10$ , (B)  $m = 1:20$ , (C)  $m = 1:50$ , (D)  $m = 1:100$ , and several wave conditions, case 1 (solid line), 2 (dashed-dot line) and 3 (small dotted line). The large dots represent the total sediment transport with no seawall.

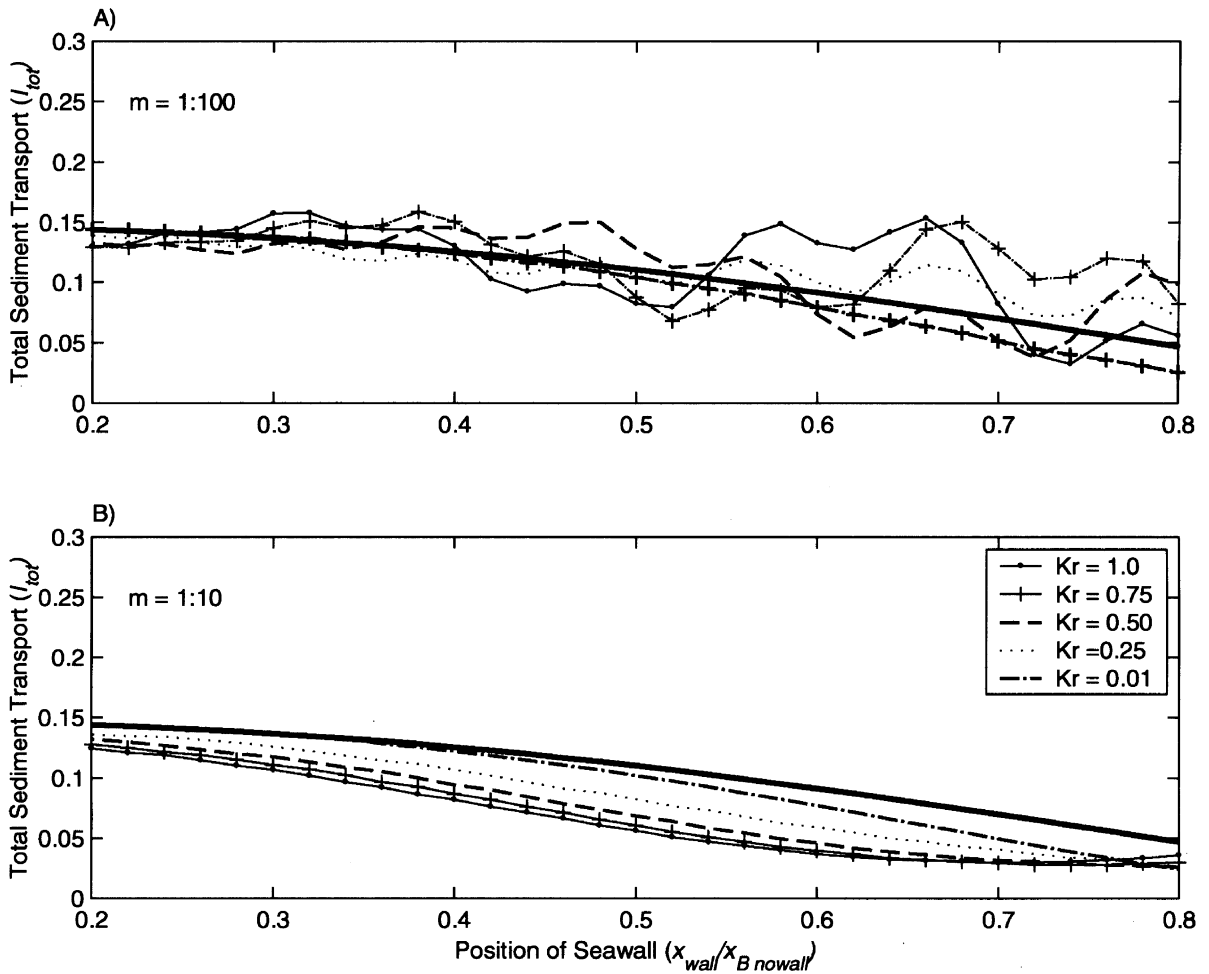


Fig. 10. Effect of the reflection coefficient on total sediment transport for two planar beach slopes (A)  $m = 1:100$ , (B)  $m = 1:10$  and five reflection coefficients,  $K_r = 1.0$  (small dots on thin solid line),  $0.75$  (plusses on thin solid line),  $0.50$  (dashed line),  $0.25$  (small dotted line) and  $0.01$  (dash-dot line). The thick solid line represents the total sediment transport with no seawall.

surf zone. For the steep sloping beach (Fig. 10B), increasing the reflection coefficient actually decreases the total sediment transport for most positions of the seawall. For both beaches, the model shows the total sediment transport tending toward the no wall solution as the reflection coefficient goes to zero.

## 5. Discussion

In the following section, solving the linear long wave equation analytically with a seawall as the

landward boundary condition both confirms some of the results of the present model and illustrates the complex behaviour of alongshore processes fronting a seawall. A discussion of practical considerations concerning the seawall problem follows.

### 5.1. The long wave equation

The solution for the free surface profile in front of a seawall, from the long wave equation, is a combination of Bessel functions. In Fig. 11A, a dimensionless amplification factor,  $\bar{\eta}/d_{B \text{ no wall}}$ , from the long wave equation is compared to the solution of the

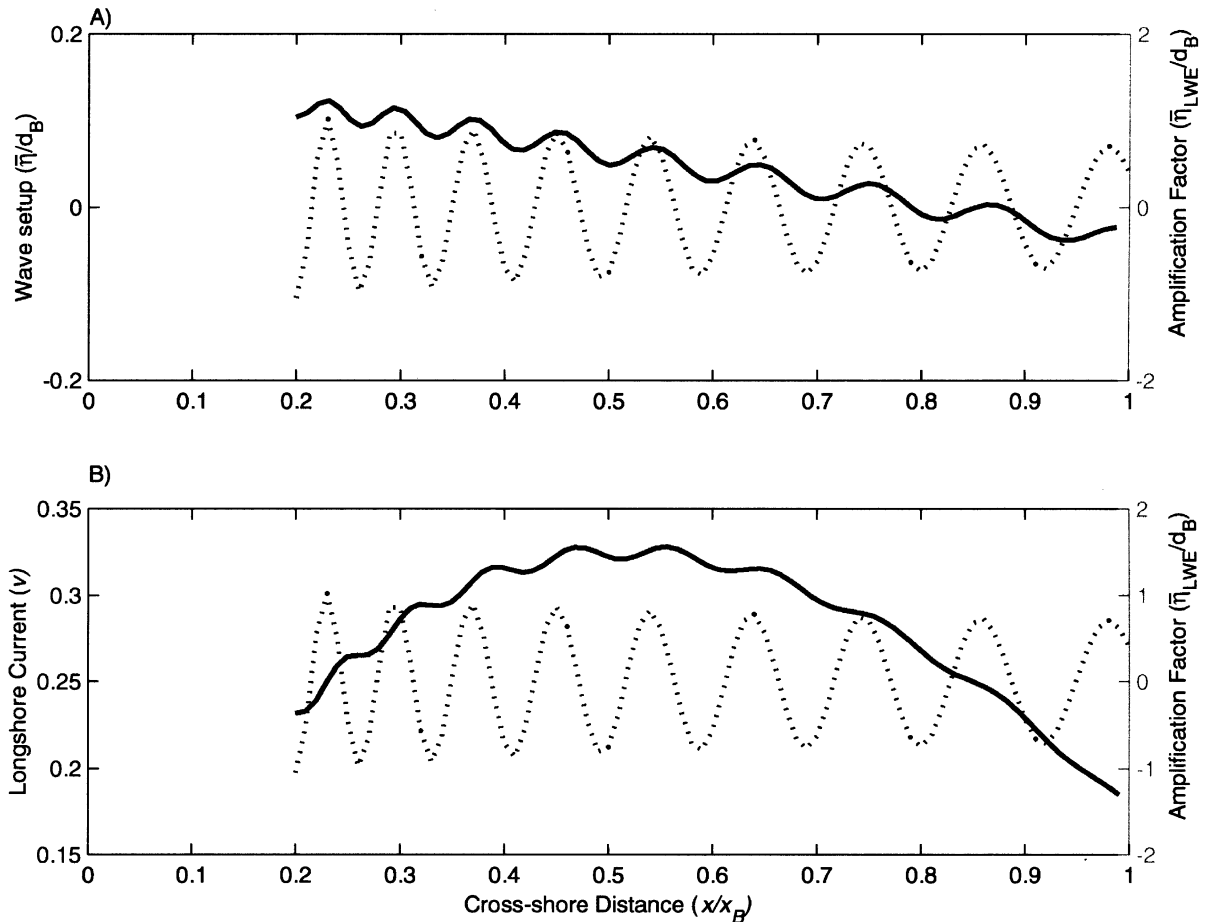


Fig. 11. (A) Comparison between the wave setup in front of a seawall (solid line), case 3d, and the linear long wave equation (dotted line). (B) Comparison between the longshore current fronting a seawall (solid line) and the linear long wave equation (dotted line).

cross-shore equation of motion (Eq. (14)). Although the magnitudes of the two solutions are quite different (note the different scales on the vertical axes), the similarity in the modulations of the free surface is apparent. The results presented in this figure were calculated for case 3d with the seawall at 20% of the no wall surf zone width,  $x_{\text{wall}}/x_{B \text{ no wall}} = 0.2$ . Similar results have been reproduced for all cases. Comparing the long wave amplification factor to the longshore current profile (Fig. 11B) again reveals that there is a one-to-one correspondence between the modulations of the two models.

Due to the Bessel function nature of the solution to the long wave equation, as the seawall is moved seaward the linear long wave equation encounters

singularities that result in free surfaces with infinite magnitudes. The larger the surf zone width, the more singularities. Earlier, it was shown that the maximum longshore current for case 3d occurs when the seawall is at a cross-shore position of approximately three-fifths of the no wall surf zone width ( $x_{\text{wall}}/x_{B \text{ no wall}} = 0.63$ ). This corresponds almost exactly to one of the singularities in the long wave equation and may help to explain the results of Jones (1975) who found that maximum erosion occurred when the seawall was located three-fifths of the distance from the still water line to the break point. Fig. 12 shows the maximum longshore current as a function of the seawall location for cases 3c and 3d. The singularities in the long wave equation (indicated as pluses

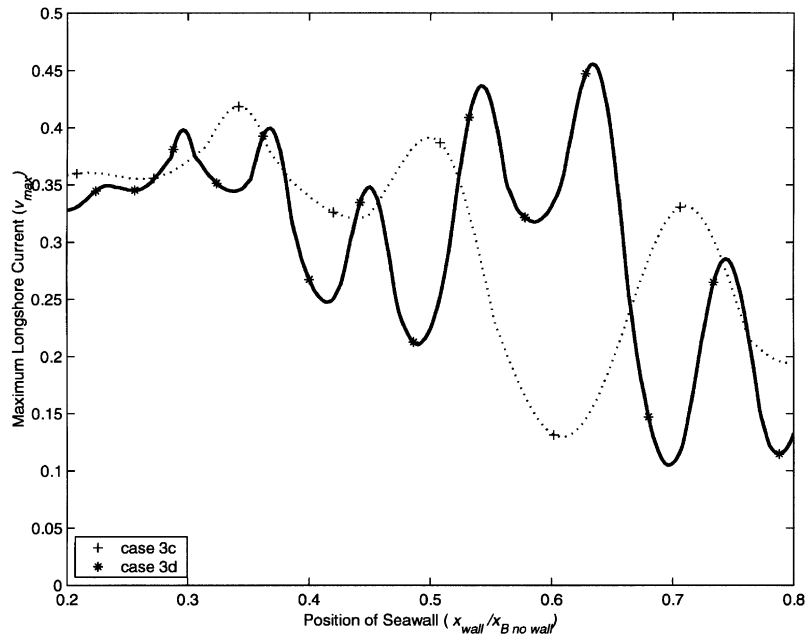


Fig. 12. Singularities of the long wave equation (pluses and asterisks) superimposed on the maximum longshore current (dashed line and solid line) for cases 3c and 3d, respectively, and many positions of the seawall.

and asterisks) fall exclusively on or near the local maxima and minima in these curves. These results are somewhat surprising as we are comparing a cross-shore quantity from a fairly simple model with longshore quantities from a more complex model. It does, however, suggest that the behaviour of the longshore current and sediment transport in front of a seawall can be explained in terms of a resonance, which is tuned by the position of the seawall across the surf zone.

### 5.2. Practical considerations

The solution to the long wave equation helps to explain some of the sensitivity of the model results shown earlier, such as the great affect that seawall position has on the longshore current and sediment transport. Much of this sensitivity is of course an artifact of forcing the model with monochromatic waves. Random waves, as experienced in nature, would serve to damp the singularities and smooth the behaviour of the response. However, it is expected that the cross-shore position of the seawall would

still non-linearly affect the longshore current and sediment transport fronting the wall.

The longshore current and suspended sediment data reported by Miles et al. (2001) consist of only 1 day of measurements and thus only one cross-shore location of the seawall relative to incident wave conditions. The fairly low energy conditions during their experiment and the moderately sloped beaches of the site most closely resemble case 1b of the present model. As shown in Fig. 7b, this is the lone scenario in which the modeled longshore currents and sediment transport are clearly and consistently higher than the no seawall situation. This may help to explain why Miles et al. (2001) measured higher sediment transport rates in front of the seawall than on the adjacent natural beach. The present study may also suggest that under different hydrodynamic and morphologic conditions (different beach slope), the in situ measurements of Miles et al. (2001) may have resulted in the opposite conclusions, such as those proposed by Rakha and Kamphuis (1997a,b), regarding the influence of seawalls on longshore currents and sediment transport.

What remains clear is that the debate about the influence of seawalls on beaches has not been resolved. However, the results of the present study indicate potential mechanisms resulting in the contradictions in the available seawall literature. Obviously, rigorous field measurements at a variety of sites with differing morphologic and hydrodynamic characteristics as well as physical and numerical modeling efforts are still necessary to provide much needed insight into the seawall problem. The effect of seawalls on beaches appears to be most sensitive to the position of the seawall within the surf zone, the beach slope, and the reflection coefficient, and future work should investigate these parameters in detail.

## 6. Conclusions

An analytic model has been developed to estimate wave setup, longshore currents, and the associated sediment transport on a planar beach backed by a seawall. The model assumes shallow water, small angle of wave incidence, spilling breakers, and conservation of reflected wave energy flux. A partial standing wave develops in front of the seawall causing modulations in the bottom shear stress, radiation stress, setup/setdown, longshore current, and longshore sediment transport. Modulations associated with the total water depth and bottom stress are relatively small and can be neglected. The modulation of the radiation stress is retained and forces longshore current and sediment transport profiles, which behave quite differently than no seawall formulations.

Reflection from a seawall causes waves to break further seaward, resulting in a steeper total water depth slope. However, the effective width of the surf zone (the distance from the seawall to the break point) is actually less than the surf zone width without a seawall. As the reflection coefficient goes to zero, the present model collapses to the classical no seawall solutions for wave setup, longshore current and sediment transport on planar beaches. The magnitudes of the longshore current and sediment transport in front of a seawall can be either greater than or less than a similar beach without a seawall depending on the location of the seawall in the surf

zone for particular choices of beach slope and wave conditions. A comparison with the solution to the linear long wave equation suggests that the position of the seawall serves to tune the surf zone with some positions forcing a resonant condition causing local maxima and minima in the behaviour of the integrated longshore current and sediment transport.

### List of notation

$\alpha$	slope of setup
$\gamma$	non-dimensional ratio of depth at breaker line to deep water wavelength
$\varepsilon_r$	phase between incident and reflected wave
$\varepsilon'_r$	cross-shore derivative of phase between incident and reflected wave
$\varepsilon_{rg}$	geometric component of phase
$\varepsilon_{rw}$	wave component of phase
$\eta$	free-surface elevation
$\theta$	wave angle
$\theta_i$	incident wave angle
$\theta_r$	reflected wave angle
$\kappa$	breaker index
$\mu_e$	eddy viscosity
$\pi$	pi (numerical constant)
$\rho$	mass density of water
$\sigma(x)$	spatially dependent phase term
$\tau_b$	bottom stress
$\tau_{by}$	longshore component of bottom stress
$\Phi$	total velocity potential
$\phi_i$	incident velocity potential
$\phi_r$	reflect velocity potential
$\psi$	constant
$\omega$	wave angular frequency
$A$	constant proportional to reflected wave energy flux
$a_i$	incident wave amplitude
$a_r$	reflected wave amplitude
$C$	wave celerity
$c_1$	constant of integration
$c_2$	orbital velocity coefficient
$c_3 \dots c_7$	non-dimensional coefficients
$C_B$	non-dimensional break point celerity
$C_f$	dimensionless bottom stress coefficient
$C_{gr}$	reflected wave group velocity
$d$	total water depth
$E_{ii}$	incident wave energy
$E_{ir}$	cross wave energy
$E_{rr}$	reflected wave energy

$f$	spatial oscillation term
$F_i$	incident wave energy flux
$F_r$	reflected wave energy flux
$g$	acceleration due to gravity
$g(z)$	depth dependent coefficient
$h$	still water depth
$I$	sediment transport rate
$I_{\text{tot}}$	total sediment transport
$k$	wave number
$K_r$	reflection coefficient
$L_0$	deep water wavelength
$n$	ratio between group velocity and celerity
$N$	dimensionless constant
$P$	lateral mixing coefficient
$Q_{\text{tot}}$	total volumetric flow rate
$s$	total slope
$s_{\text{MH83}}$	total depth slope of no wall solution
$S_{xx}$	cross-shore component of onshore radiation stress
$S_{xy}$	longshore component of onshore radiation stress
$T$	wave period
$u$	total depth averaged velocity vector
$u_x$	cross-shore component of wave orbital velocity
$u_y$	longshore component of wave orbital velocity
$v$	mean longshore current
$V_h$	homogeneous solution to Euler equation
$x_o$	offshore location

### Subscripts

$O_B$	values calculated at breaker line
$O_{B \text{ eff}}$	values calculated at the effective breaker line
$O_{B \text{ no wall}}$	values calculated at no wall breaker line
$O_{\text{wall}}$	values calculated at location of seawall

### Superscripts

$()^*$	dimensional quantity
--------	----------------------

### Acknowledgements

We would like to thank Paul Komar, Nathaniel Plant, and three anonymous reviewers for carefully

reviewing this manuscript and providing many helpful suggestions. Funding for this work was partially provided by the NOAA office of Sea Grant.

### References

- Bagnold, R.A., 1963. Beach and nearshore processes: Part I. Mechanics of marine sedimentation. In: Hill, M.N. (Ed.), The Sea. Interscience, New York, pp. 507–528.
- Birkemeier, W.A., 1980. The effects of structures and lake level on bluff and shore erosion in Berrigen County, Michigan, 1970–1974, Miscellaneous Report No. 80-2, Coastal Engineering Research Center, US Army Corps of Engineers, 74 pp.
- Bowen, A.J., Inman, D.L., Simmons, V.P., 1968. Wave set-down and set-up. Journal of Geophysical Research 73, 2569–2577.
- Bowen, A.J., 1969. The generation of longshore currents on a plane beach. Journal of Marine Research 27, 206–215.
- Dean, R.G., 1986. Coastal armoring: effects, principles, and mitigation. Proceedings 20th Coastal Engineering Conference, American Society of Civil Engineers, 1843–1857.
- Fletcher, C.H., Mullane, R.A., Richmond, B.M., 1997. Beach loss along armored shorelines on Oahu, Hawaiian Islands. Journal of Coastal Research 13 (1), 209–215.
- Griggs, G.B., Tait, J.F., 1990. Beach response to the presence of a seawall, a comparison of field observations. Shore and Beach, 11–28.
- Griggs, G.B., Tait, J.F., Corona, W., 1994. The interaction of seawalls and beaches: seven years of monitoring, monterey bay, California. Shore and Beach, 21–28.
- Hearon, G.E., McDougal, W.G., Komar, P.D., 1996. Long-term beach response to shore stabilization structures on the Oregon coast. Proceedings 25th Coastal Engineering Conference, American Society of Civil Engineers, 2718–2731.
- Jones, B., Basco, D.R., 1996. Seawall effects on historically receding shorelines. Proceedings 25th Coastal Engineering Conference, American Society of Civil Engineers, 1985–1997.
- Jones, D.F., 1975. The Effect of Vertical Seawalls on Longshore Currents, unpublished PhD Thesis, Department of Coastal and Oceanographic Engineering, University of Florida, Gainesville, FL, 188 pp.
- Kraus, N.C., 1987. The effects of seawalls on the beach: a literature review. Proceedings Coastal Sediments '87, American Society of Civil Engineers, 945–960.
- Kraus, N.C., McDougal, W.G., 1996. The effects of seawalls on the beach: Part I. An updated literature review. Journal of Coastal Research 12 (3), 691–701.
- Kraus, N.C., Smith, J.M., Sollitt, C.K., 1992. SUPERTANK Laboratory Data Collection Project. Proceedings 23rd Coastal Engineering Conference, American Society of Civil Engineers, 2191–2204.
- Longuet-Higgins, M.S., 1970a. Longshore currents generated by obliquely incident sea waves, 1. Journal of Geophysical Research 75, 6778–6789.
- Longuet-Higgins, M.S., 1970b. Longshore currents generated by obliquely incident sea waves, 2. Journal of Geophysical Research 75, 6790–6801.

- Macdonald, H.V., Patterson, D.C., 1984. Beach response to coastal works Gold Coast, Australia. Proceedings 19th Coastal Engineering Conference, American Society of Engineers, 1522–1538.
- McDougal, W.G., Hudspeth, R.T., 1983a. Wave setup/setdown and longshore currents on non-planar beaches. *Coastal Engineering* 7, 103–117.
- McDougal, W.G., Hudspeth, R.T., 1983b. Longshore sediment transport on non-planar beaches. *Coastal Engineering* 7, 119–131.
- McDougal, W.G., Hudspeth, R.T., 1986. Influence of lateral mixing on longshore currents. *Ocean Engineering* 13, 4199–4433.
- McDougal, W.G., Kraus, N.C., Ajiwibowo, H., 1996. The effects of seawalls on the beach: Part II. Numerical modelling of SUPERTANK seawall tests. *Journal of Coastal Research* 12 (3), 702–713.
- Miles, J.R., Russel, P.E., Huntley, D.A., 2001. Field measurements of sediment dynamics in front of a seawall. *Journal of Coastal Research* 17 (1), 195–206.
- Plant, N.G., Griggs, G.B., 1992. Interactions between nearshore processes and beach morphology near a seawall. *Journal of Coastal Research* 8 (1), 183–200.
- Rakha, K.A., Kamphuis, J.W., 1997a. Wave induced currents in the vicinity of a seawall. *Coastal Engineering* 30, 23–52.
- Rakha, K.A., Kamphuis, J.W., 1997b. A morphology model for an eroding beach backed by a seawall. *Coastal Engineering* 30, 53–75.
- Ruggiero, P., 1997. Wave Runup on High Energy Dissipative Beaches and the Prediction of Coastal Erosion, PhD Dissertation, Oregon State University, Corvallis, OR, 145 pp.
- Silvester, R., 1977. The role of wave reflection in coastal processes. Proceedings Coastal Sediments '77, 639–654.
- Thornton, E.B., Guza, R.T., 1986. Surf zone longshore currents and random waves: field data and models. *Journal of Physical Oceanography* 16 (7), 1165–1178.
- Weggel, J.R., 1988. Seawalls: the need for research, dimensional considerations and a suggested classification. In: Kraus, N.C., Pilkey, O.H. (Eds.), *The Effects of Seawalls on the Beach*. *Journal of Coastal Research*, SI 4, pp. 29–40.